INFLUENCE OF MICROSTRUCTURE ON SMALL CRACK GROWTH BEHAVIOUR OF MARAGING STEEL WELD

Haitao Zhao, Delun Guo

Aeronautical Key Laboratory for Welding and Joining Technologies, AVIC Manufacturing Technology Institute, Beijing

Abstract: Experiments were carried out to study the influence of microstructure on fatigue small crack growth behaviour of 18Ni maraging steel and weld. Microstructure characteristics of weld metal and base metal were analyzed by optical microscope and scanning electron microscope. Results show that the microstructure of weld metal and base metal mainly includes matrix of lath martensite and dispersed nano-sized particles of $Ni_3(Mo,Ti)$ strengthening phase in matrix. And massive reversed austenite phases exist only in the interdendritic region of weld metal, where the elements of Mo, Ti are enriched. Fatigue tests show that there are extremely less fatigue cycles required for crack initiation and growth at the surface defect of weld metal under the condition of higher fatigue loading value, compared with base metal. Furthermore, compared with base metal, fatigue small crack growth rate of weld metal with microstructure characteristics of larger size of block grains and lower density of high-angle boundaries and low-angle boundaries is significantly faster than that of base metal, and the discrepancy between them is even more obvious near the threshold.

Keywords: small crack growth, microstructure, weld metal, base metal, 18Ni maraging steel

INTRODUCTION

Defects or damages inevitably appear in metal structures during engineering manufacture and during service, where fatigue cracks often occur and extend to structural failure under cyclic loading. Therefore, the researches on fatigue crack growth behaviour have always been an important part of structural durability analysis. Especially, a large number of researches have revealed that microstructure characteristics of metal materials have significant influences on small crack growth behaviour. For example, firstly, compared with fine grains, coarse grains can accommodate a large number of dislocations along the slip planes, resulting in great mechanical stress acting on the dislocation sources in the adjacent grains, which consequently promotes the transmission of plasticity and crack across the grain boundaries [1,2]. Secondly, high-angle boundaries can provide higher potential boundary barriers in metal materials, which results in that small crack tends to observably slow down or even stop under low ΔK when approaching or transferring high-angle boundaries, while low-angle grain boundaries have little effect on crack growth rate[3,4,5]. Thirstly, the intrinsic resistance of a grain boundary depends on the twist misorientation angle ξ within the grain boundary plane and the structure of the grain boundary itself, which makes it easier for the grain boundaries with a large twist component to arrest or branch short crack [2,6-9]. In addition, in duplex steels, small

crack grow faster in the "soft phase" with low yield strength than in the "hard phase" with high yield strength, and when it extend to the boundaries from soft phase to hard phase, the crack growth rate slows down or stops[10-14].

Various welded structures of high-strength steel have been gradually spreading to application of aviation load-bearing parts. In engineering applications, micro-defects in weld metal often lead to the fatigue failure of welded structures of high-strength steel, and severe microstructure heterogeneity of weld metal also affects the fatigue crack growth behaviour. However, the researches on crack growth behaviour of weld metal of high-strength steel have been more focused on long crack growth performance, while small crack growth behaviour of weld metal has been lack of understanding[15-18]. This paper takes 18Ni maraging steel as the object to analyze the effect and mechanism of microstructure characteristics of weld metal on small crack growth behaviour.

EXPERIMENTAL PROCEDURES

Table 1: Major chemical compositions of 18Ni maraging steel (wt %)

C	*Ni*	*Mo*	*Co*	*Cr*	*Si*	*Ti*	*Al*	*Mn*	*S*	*Cu*	*Fe*
≤0.02	17.50～19.00	4.60～5.20	7.50～8.50	≤0.5	≤0.10	0.30～0.50	0.05～0.15	≤0.10	≤0.007	≤0.5	matrix

The experimetal material is 18Ni maraging steel, which is a kind of super-strength steel with ultra-low carbon and Fe-Ni martensite matrix. As-forged, major chemical components are shown in Table 1. The specimens were welded by argon tungsten arc welding method. Then the welded specimens were put into a vacuum furnace for solution treatment and subsequent aging treatment. The parameters of solution treatment are holding at 830℃ for 1.5 hours and air cooling, in order to obtain Fe-Ni martensite matrix. The parameters of aging treatment are holding at 480℃ for 4.5 hours and air cooling, in order to dispersely precipitate strengthening phases of Ni_3 (Mo, Ti) in martensite matrix.

Metallographic samples also were taken from the welded specimen. After that, the morphologies of metallographic samples were etched out with 4% nitric acid alcohol solution. Microstructure characteristics of all of the samples were observed by LeicaDM5000 optical metallographic microscope (OM) and JSM7900F scanning electron microscope (SEM) respectively. Element contents of major phases were analyzed by energy spectrum method, and micro-grain orientation maps were analyzed by selected area electron backscattering diffraction (EBSD).

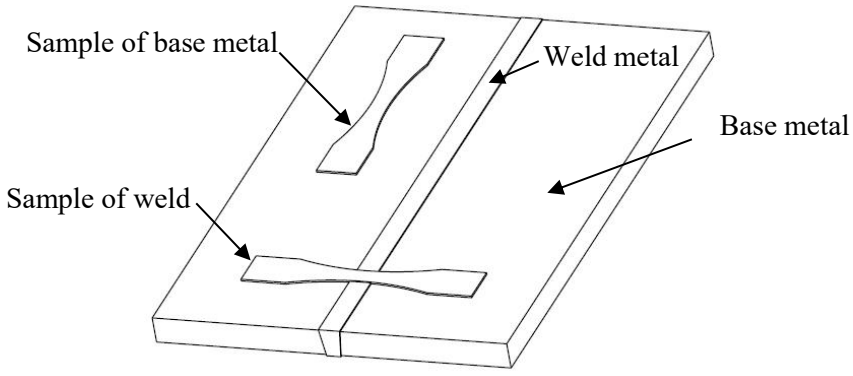

Figure 1: Schematic diagram of sampling position of small crack test sample

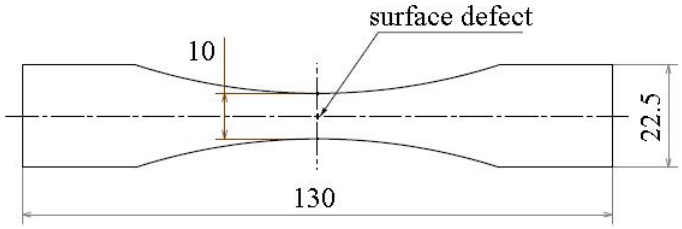

Figure 2 Schematic diagram of fatigue sample with small crack

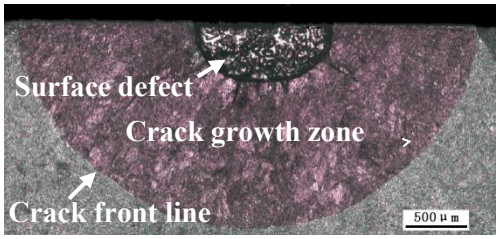

Figure 3 Fracture morphology of the sample of surface crack propagation

As shown in Figure 1, fatigue samples for weld metal and base metal were taken from welded specimen with the thickness of 2.5mm. Figure 2 shows the schematic diagram of the shape and size of fatigue sample. And surface defect with length of about 0.6mm, width of about 0.1mm and depth of about 0.4mm was prefabricated at the center of the fatigue sample surface by the method of laser processing. Cyclic loading with constant value was adopted to initiate fatigue crack at defect. As described in reference [19], surface crack generally grows in the length direction and the depth direction in an approximate semi-elliptical shape. By analyzing the crack front line of the fracture of several fatigue samples in the experiment, shown in Figure 3, the ratio value of depth c to length a during the crack growth was determined to be 0.8 for 18Ni maraging steel. Additionally, crack length was measured by optical microscope during fatigue test.

The fatigue crack growth behaviour was tested on the QBG-100 high-frequency fatigue testing machine, under the conditions of constant-value loading value, the frequency of 100Hz and the stress ratio of 0.1. Equation (1) was used to calculate the magnitude of stress intensity factor of fatigue small crack, as shown in the following formula[20].

$$\Delta K = \Delta S_t \times \sqrt{\frac{\pi a}{Q}} \times F\left(\frac{a}{t}, \frac{a}{c}, \frac{c}{b}, \emptyset\right) \quad (1)$$

$$Q = 1 + 1.464 \times (a/c)^{1.65} \quad (2)$$

Here, ΔS_t is the far-field stress amplitude, a is the crack depth, c is the half of crack length, F is the shape factor, t is the thickness of fatigue sample, b is the width of fatigue sample, and $\varnothing$ is the elliptical parametric angle.

EXPERIMENTAL RESULTS AND DISCUSSION

Microstructure characteristics

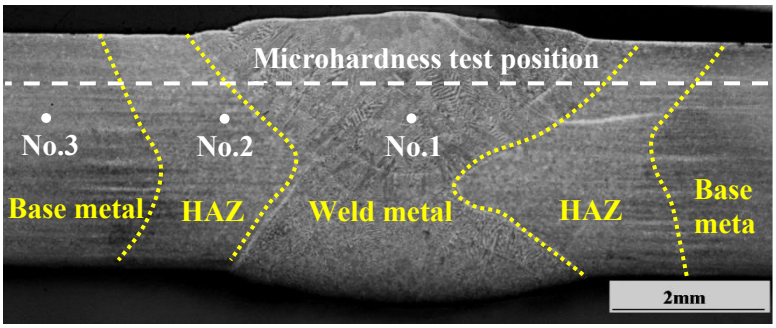

Figure 4 Macro-morphology of 18Ni maraging steel weld

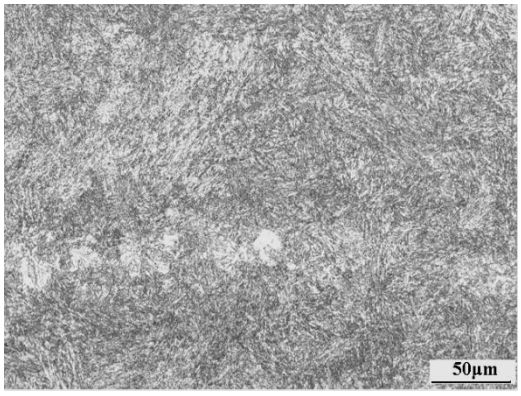

(a) Base metal (Postion No.3 in Fig.4)

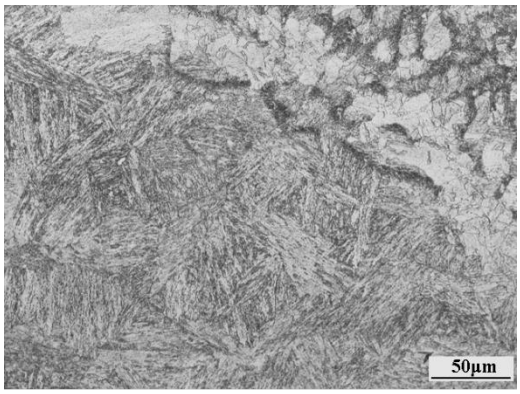

(b) Heat affected zone (Postion No.2 in Fig.4)

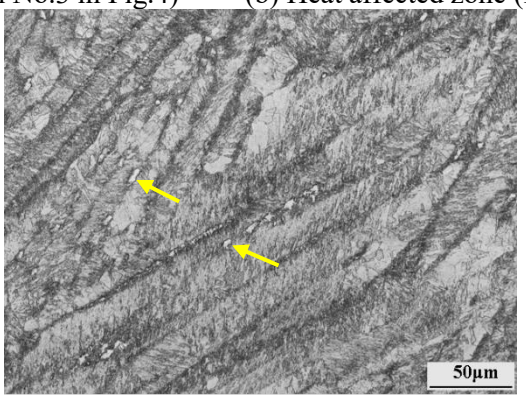

(c) weld metal (Postion No.1 in Fig.4)

Fig.5 Morphologies of microstructure of 18Ni maraging steel weld

The 18Ni steel weld consists of weld metal, heat affected zone (HAZ) and base metal, as shown in Figure 4. Generally, base metal is not affected by welding heat, and its microstructure characteristics are consistent with those of raw material. The optical microstructures of base metal include equiaxed prior austenite grains with the average size of about 28.2μm and fine lath martensite phases inside them, as shown in Figure 5(a). Weld metal refers to the material of the area that is melted and subsequently solidified by welding heat. The optical microstructures of weld metal include dendrite with the average width of about 16μm and fine lath martensite inside them and some massive reversed austenite distributed in the interdendrites, as indicated by arrows in Figure 5(c). Heat affected zone (HAZ) is located between weld metal and base metal with coarse prior austenite grain of the average size of about 71.5μm and lath martensite inside them near weld fusion line, as shown in Figure 5(b).

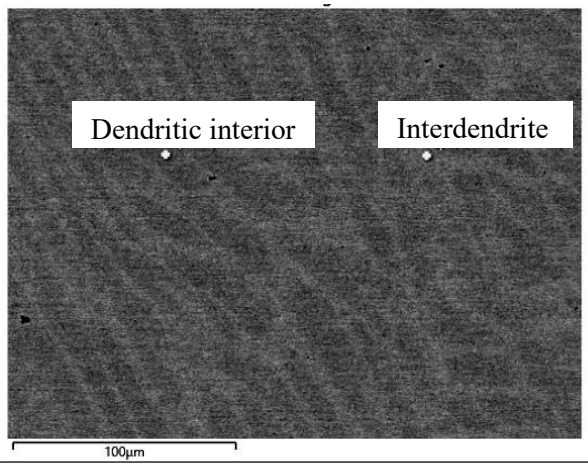

Test position	*Ni*	*Mo*	*Co*	*Ti*	*Fe*
interdendrite	19.34	1.30	8.39	0.79	70.18
dendritic interior	17.51	0.05	8.37	0.31	73.76

Noting: the atomic percentage is calculated after minor elements are not included.

Figure 6 Energy spectrum analysis results of major elements of interdendrite and dendritic interior in weld metal

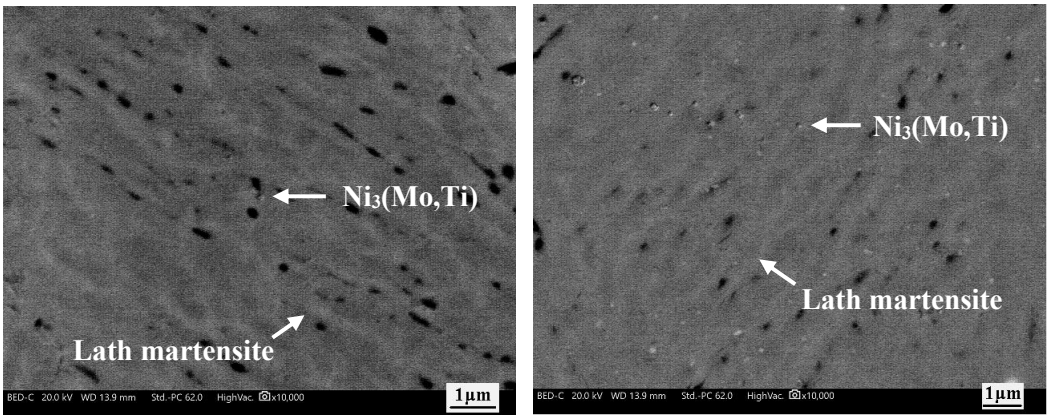

(a) weld metal (b) base metal

Figure 7 Morphologies of strengthening phases precipitated dispersely among lath martensite matrix, part of strengthening phases were eroded away to form cavities

Figure 6 reveals that the contents of Mo and Ti in the region of interdendrites is significantly higher than those in the region of dendritic interior in weld metal, which is due to the segregation of these elements to interdendrites during solidification of weld metal. As pointed out in Reference [21,22], metastable martensite in maraging steel is prone to reverse phase transformation in Mo and Ti-rich areas during aging treatment, forming massive reversed austenite, as indicated by the arrow in Figure 5(c). Additionally, it can be found through high magnification SEM photos that precipitation strengthening phases $Ni_3(Mo,Ti)$ are dispersed among lath martensite matrix in the form of nano-sized fine particles in weld metal and base metal, as shown in Figure 7.

Crack growth behaviour of base metal

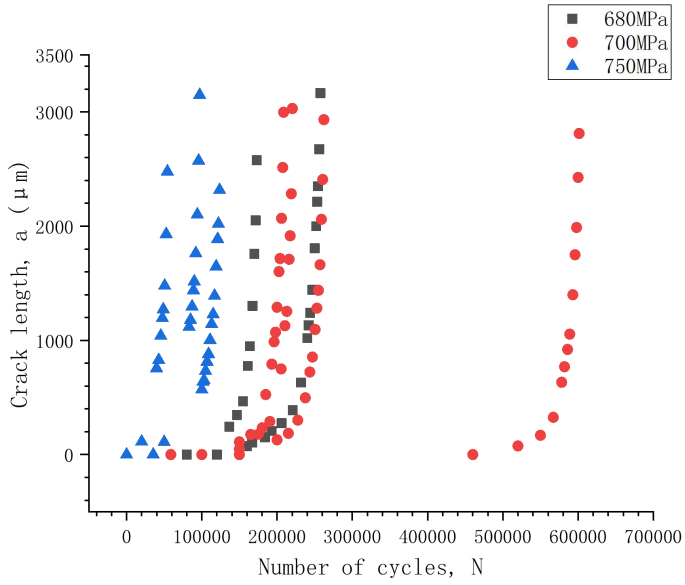

Figure 8 Crack length vs. Number of fatigue cycles for base metal

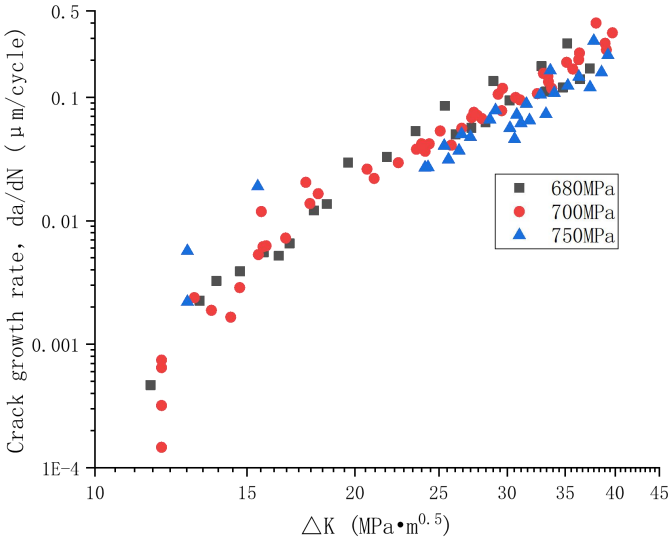

Figure 9 Fatigue crack growth rate vs. stress intensity range at stress ratio R=0.1 for base metal

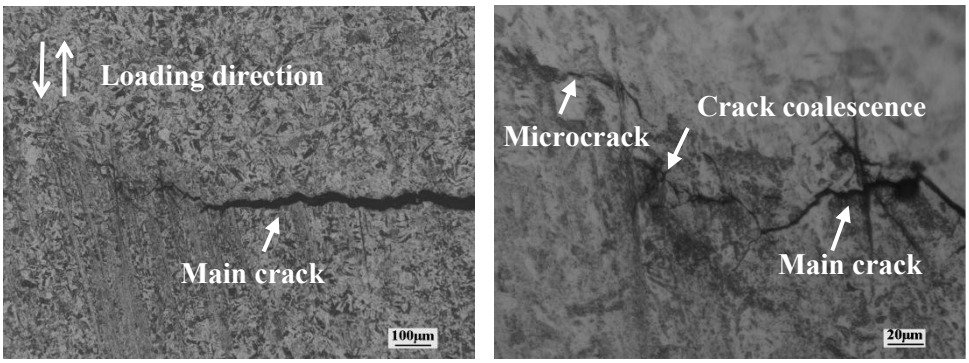

(a) main crack growth path (b) microcracks and crack coalescence

Figure 10 Morphologies of small crack growth path of the sample of base metal under the condition of fatigue loading value of 680MPa and cyclic number of 257600 cycles

The fatigue crack growth behaviour of base metal was tested under the condition of constant loading values of 680MPa, 700MPa and 750MPa respectively, which are slightly lower than fatigue limit of 18Ni material. Figure 8 showed that fatigue cycles under the condition of loading value of 750MPa were significantly smaller than those under the condition of loading value of 680MPa and 700MPa to initiate fatigue crack at surface defect. Moreover, once initiation crack started to crack, the tests under the condition of loading value of 750MPa required less fatigue cycles than those under the condition of the loading value of 680MPa and 700MPa to reach the stage of rapid crack growth. Obviously, the larger the fatigue loading value is, the more beneficial it is to initiate fatigue crack at surface defect, and the earlier it tends to reach accordingly the stage of rapid crack growth. Figure 9 demonstrated that the data distributions of small crack growth rate vs. ΔK of base metal were similar to those of long crack growth rate vs. ΔK in the near-threshold region [23,24]. Moreover, test data of small crack growth of base metal under the conditions of three loading values have little dispersion.

Additionally, under the condition of fatigue loading values of 750MPa, slightly lower than the fatigue limit of 18Ni material, quite a few independent microcracks were also initiated at the boundaries of grains or phases on the surface of base metal samples, as shown in Figure 10. Generally, under the condition of high cycle fatigue, the behaviours of independent microcracks initiation and crack coalescence determine the early stage of fatigue life [25]. Thereafter, during the main crack growth, the coalescence effect between main crack and some microcracks near the main crack tip inevitably occur, which leads to the increasing of main crack growth rate. Especially, the crack coalescence effect is universally influenced by important factors such as the angle between the straight line connecting the two crack tips and the loading axis, and the critical distance between the crack tips [26,27,28].

Crack propagation behaviour of weld metal

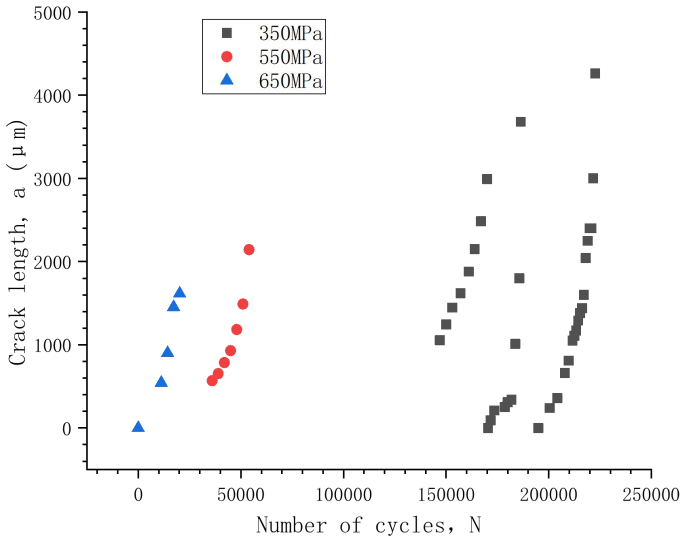

Figure 11 Crack length vs. Number of fatigue cycles for weld metal

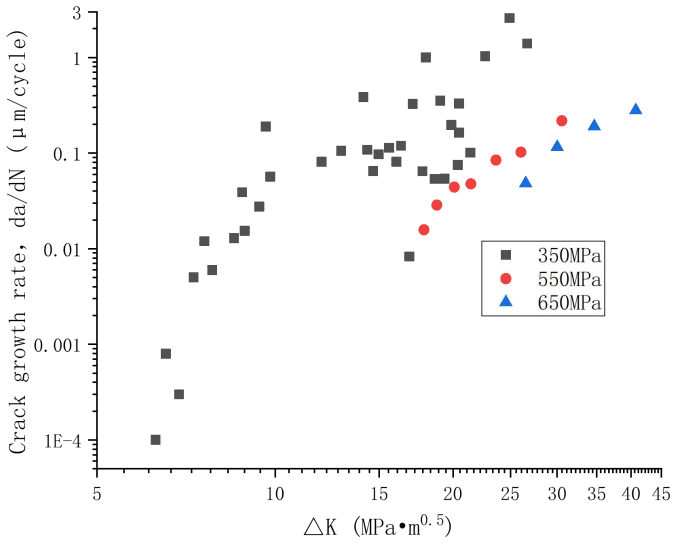

Figure 12 Fatigue crack growth rate vs. stress intensity range at stress ratio R=0.1 for weld metal

The fatigue crack growth behaviour of weld metal was tested under the condition of constant loading values of 550MPa and 650MPa which are lower than fatigue limit of 18Ni material, and constant loading value of 350MPa which is far below fatigue limit of 18Ni material. Although the effective test data of fatigue crack growth behaviour of weld metal were limited, it can still be found from Figure 11 that there were extremely less fatigue cycles required for crack initiation and growth at the surface defects of weld metal samples under the conditions of fatigue loading of 550MPa and 650MPa, compared with base metal samples under the conditions of fatigue loading of 680MPa and 700MPa. Moreover, only under the condition of fatigue loading of 350MPa were there more fatigue cycles to initiate fatigue crack. Meanwhile, there were less fatigue cycles for crack growth for weld metal under the condition of fatigue loading of 350MPa than those of base metal under the fatigue loading of 680MPa and 700MPa. Figure 12 demonstrated that effective test data at the lower △K were available, only under the condition of fatigue loading of 350MPa, while effective data presented great dispersion at the higher △K under the fatigue loading under the same condition.

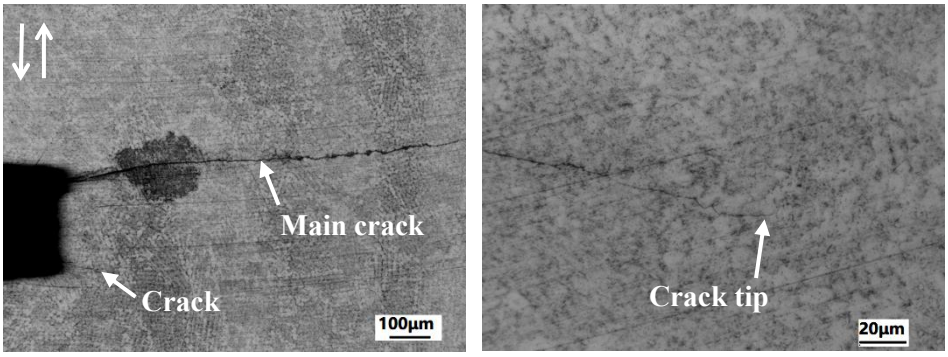

(a) main crack path (b) crack tip

Fig.13 Morphologies of small crack growth path of the sample of weld metal under the condition of fatigue loading value of 350MPa and cyclic number of 170000 cycles

Under the condition of fatigue loading value far below the fatigue limit of 18Ni material, there were almost no microcracks along crack growth path on the surface of weld metal sample, as shown in Figure 13. Additionally, there existed several cracks at surface defect, and the main crack grew along the direction perpendicular to the loading direction, mainly in transgranular mode while other cracks did not grow further. Consequently, fatigue crack growth rate of weld metal is mainly determined by

the interaction between crack driving force of the main crack tip and microstructure, and no other cracks or microcracks are involved.

Discussion

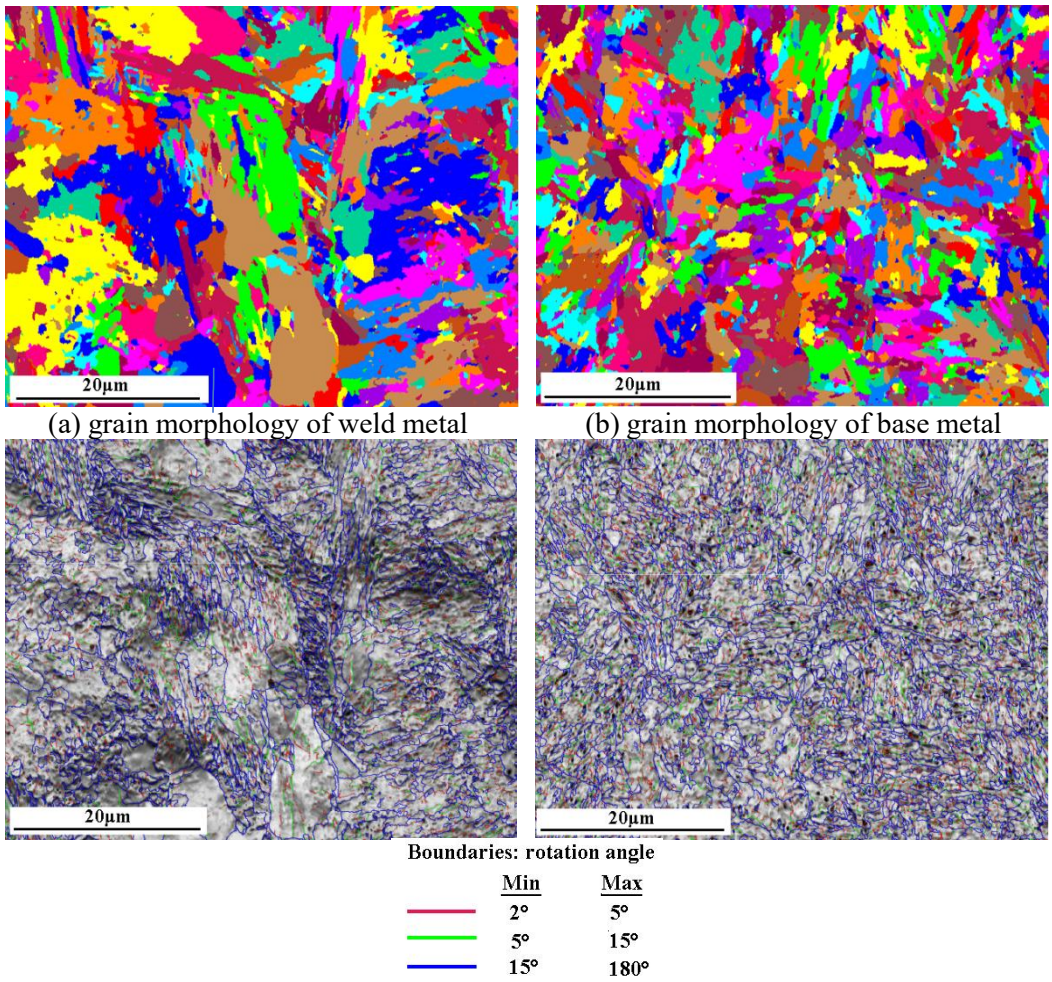

(a) grain morphology of weld metal (b) grain morphology of base metal

(c) boundary orientation of weld metal (d) boundary orientation of base metal

Figure 14 Grain morphologies and boundaries orientation of weld metal and base metal measured by EBSD

Table 3: Statistical results of various types of boundaries distribution (Photos in Fig.14 (c) and (d))

Rotation angle / *Material type*	*2°~15°*			*15°~180°*	
	Number	*Length (mm)*	*Density (number/m²)*	*Number*	*Length (mm)*
Weld metal	38086	2.20	16.10×10^6	77763	4.49
Base metal	56602	3.26	23.93×10^6	93572	5.40

It has been reported that block grain is the basic microstructure unit controlling the strength and fracture of lath martensite in maraging steel, which is expected to act as barriers of moving dislocations during the deformation of lath martensite structure [29,30,31]. Figure 14(a) and (b) show the distribution of block grains in weld metal and base metal of 18Ni maraging steel, in which a color represents a single block grain. Obviously, the average size of block grains of weld metal which is about 6.17μm is significantly larger than that of base metal which is about 3.51μm. In addition, Figure 14(c) and (d) reveal various types of boundaries in weld metal and base metal. The statistical results of the number and length of various types of boundaries in weld metal and base metal are displayed in Table 3. Regardless of high-angle boundaries with misorientation greater than 15° or low-angle

boundaries with misorientation less than 15°, the quantity and total length in weld metal are obviously smaller than those of base metal. Correspondingly, it can also be inferred that the densities of high-angle boundaries and low-angle boundaries in weld metal are necessarily less than those in base metal.

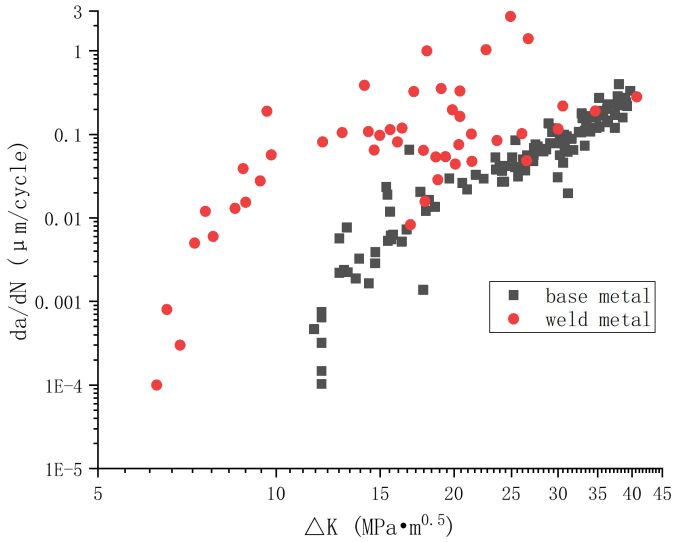

Figure 15 Comparison of fatigue crack growth behaviour between weld metal and base metal

The microstructure differences between weld metal and base metal have a great influence on fatigue small crack growth behaviour. As shown in Fig.15, fatigue small crack growth rate of weld metal is significantly faster than that of base metal, and the discrepancy between them is even more obvious near the threshold. It may be explained from two aspects. Firstly, due to the nano-sized fine particles of $Ni_3(Mo,Ti)$ dispersely coherent with the matrix in 18Ni maraging steel, it is expected that planar slip prevails and microcrack grows mainly along crystallographic slip planes. And free slip length (usually the grain size) will have an important impact on crack growth rate, that is, the longer free slip length can accommodate a larger number of dislocations, resulting in greater mechanical stress acting on the dislocation sources in the adjacent grains, and transmission of plasticity and crack across the grain boundaries is promoted [1,2]. Evidently, compared with base metal, the larger average size of block grains of weld metal is expected to lead to the larger average spacing inside block grain, and correspondingly the longer average free slip length, which can further promote the crack growth and increase the crack growth rate of weld metal. Secondly, it is well believed that high-angle boundaries can provide potential boundary barriers in metal materials. When approaching or transferring high-angle boundaries, fatigue crack under low $\triangle K$ tends to observably slow down or even stop [3,4,5]. Consequently, compared with base metal, the lower density of high-angle boundaries in weld metal, has less efficiency of microstructure barriers to crack growth, which is positive to promote the crack growth rate.

CONLUSION

(1) The microstructure characteristics of base metal is equiaxed prior austenite grains with the average size of about 28.2μm and fine lath martensite phases inside them, while the microstructure of weld metal is dendrite with the average width of about 16μm and fine lath martensite inside them and some massive reversed austenites in the interdendrites.
(2) The microstructure of weld metal and base metal mainly includes matrix of lath martensite and dispersed nano-sized particles of $Ni_3(Mo,Ti)$ strengthening phase in matrix. And massive reversed austenite phases exist only in the interdendritic region of weld metal, where the elements of Mo, Ti are enriched.

(3) The block grains of weld metal with the average of about 6.17μm are significantly larger than those of base metal with the average of about 3.51μm.
(4) Compared with base metal, fatigue small crack growth rate of weld metal with microstructure characteristics of larger size of block grains and lower density of high-angle boundaries and low-angle boundaries is significantly faster than that of base metal, and the discrepancy between them is even more obvious near the threshold.

REFERENCES

[1] E. Hornbogen, K.-H. Zum Gahr: Microstructure and Fatigue Crack Growth in a γ-Fe-Ni-Al Alloy[J]. Acta Metallurgica, 1976, 24(6): 581-592
[2] E.R. DE Los Rios, Hussain J. Mohamed, K.J. Miller. a Micro-Mechanics Analysis for Short Fatigue Crack Growth[J]. Fatigue Fract. Engng Mater. Struct. 1985, 8(1): 49-63
[3] Gemperlova, J.; Polcraova, M.; Gemperle, A.; Zarubova, N.: Synchrotron Radiation Topographic Study of Slip Transfer Across Grain Boundaries in Fe-Si Bicrystals[J]. Journal of Physics D: Applied Physics, 2006, 39(20): 4440-4449
[4] S. Zaefferer, J.-C. Kuo, Z. Zhao, M. Winning, D. Raabe: On the Influence of the Grain Boundary Misorientation on the Plastic Deformation of Aluminum Bicrystals[J]. Acta Materialia, 2003, 51(16): 4719-4735
[5] U. Krupp, W. Floer, J. Lei, Y.M. Hu, H.-J. Christ, A. Schick, C.-P. Fritzen: Mechanisms of Short-Fatigue-Crack Initiation and Propagation in a β-Ti Alloy[J]. Philosophical Magazine A,2002, 82(17-18): 3321-3332
[6] T. Zhai, X.P. Jiang, J.X. Li, M.D. Garratt, G.H. Bray. The Grain Boundary Geometry for Optimum Resistance to Growth of Short Fatigue Cracks in High Strength Al-alloys[J]. International Journal of Fatigue, 2005, 27(10): 1202-1209
[7] T.C. Lee, I.M. Robertson, H.K. Birnbaum. An In Situ Transmission Electron Microscope Deformation Study of the Slip Transfer Mechanisms in Metals[J]. Metallurgical Transactions A, 1990, 21(9): 2437-2447
[8] Y.H. Zhang Yan, Edwards Lyndon. On the Blocking Effect of Grain Boundaries on Small Crystallographic Fatigue Crack Growth[J]. Materials Science and Engineering A, 1994, 188(1-2): 121-132
[9] T. Zhai, A.J. Wilkinson, J.W. Martin. A Crystallographic Mechanism for Fatigue Crack Propagation through Grain Boundaries[J]. Acta Materialia, 2000, 48(20): 4917-4927
[10] R. Pippan, K. Flechsig, F.O. Riemelmoser. Fatigue Crack Propagation behaviour in the Vicinity of an Interface Between Materials with Different Yield Stresses[J]. Materials Science and Engineering A, 2000, 283(1): 225-233
[11] R Pippan, F.O Riemelmoser. Fatigue of Bimaterials. Investigation of the Plastic Mismatch in Case of Cracks Perpendicular to the Interface[J]. Computational Materials Science, 1998, 13(1): 108-116
[12] Jacques Stolarz, Jacques Foct. Specific features of two phase alloys response to cyclic deformation[J]. Materials Science and Engineering A, 2001, 319(C): 501-505
[13] Keiro Tokaji, Takeshi Ogawa, Shuji Osako. the Growth of Microstructurally Small Fatigue Cracks in a Ferritic-Pearlitic Steel[J]. Fatigue & Fracture of Engineering Materials & Structures, 1988, 11(5): 331-342
[14] Venkateswaran, Ganesh Sundara Raman, Pathak. Short Fatigue Crack Growth Behaviour of a Ferritic Steel Weld Metal[J]. Science and Technology of Welding and Joining, 2005, 10(1): 95-102
[15] R. O. RITCHIE, V. A. CHANG, N. E. PATON. The Influence of Retained Austenite on Fatigue Crack Propagation in HP9-4-20 High Strength Alloy Steel[J]. Fatigue & Fracture of Engineering Materials & Structures, 1979, 1(1): 107-121
[16] Qixing Sun, Kejian Li, Xiaogang Li, Shao-Shi Rui, Zhipeng Cai, Jiluan Pan. Near-Threshold Fatigue Crack Growth behaviour of 10% Cr Martensitic Steel Welded Joint with 9% Cr Weld Metal in High Temperature Air[J]. International Journal of Fatigue, 2020, 137: 1-11
[17] Kwai S. Chan, Yi-Ming Pan, David Davidson, R. Craig McClung. Fatigue Crack Growth Mechanisms in HSLA-80 Steels[J]. Materials Science and Engineering A, 1997, 222(1): 1-8

[18] Xiangyu Guo, Longfei Zhao, Xia Liu, Fenggui Lu. Investigation on the Resistance to Fatigue Crack Growth for Weld Metals with Different Ti Addition in Near-Threshold Regime[J]. International Journal of Fatigue, 2019, 120: 1-11
[19] WANG Miao-miao, ZENG Yan-ping, WANG Xi-shu, XIE Xi-shan. Relationship between Surface Length and Inside Length of Fatigue Crack in Ultra-high Strength Steel[J]. Journal of Aeronautical Materials, 2009, 29(3): 102-106
[20] J.C. Newman, I.S. Raju. an Empirical Stress-Intensity Factor Equation for the Surface Crack[J]. Engineering Fracture Mechanics, 1981, 15(1-2): 185-192
[21] Huang Xiaoying, Chen Wei, Pan Tianxi, Zhao Zuoquan. Inversely Transformed Austenite Formed during Welding of 18Ni(250 Grade) Maraging Steels[J]. IRON & STEEL, 1981, 2: 60-61
[22] Chen Wei, Huang Xiaoying, Pan Tianxi etl. Effects of the Microstructure of Weld Metal on the Fracture Toughness of 18Ni Maraging Steel[J]. IRON & STEEL, 1981, 16(1): 42-46.
[23] R. Jones; R.K. Singh Raman; A.J. McMillan. Crack growth: Does microstructure play a role?[J]. Engineering Fracture Mechanics, 2018, 187: 190-210
[24] R.O. Ritchie. Influence of Microstructure on Near-Threshold Fatigue-Crack Propagation in Ultra-High Strength Steel[J]. Metal Science, 1977, August/September: 368-381
[25] J.C. Fox, R.L. Edwards, W.N. Sharpe Jr. Thin-Film Gage Markers for Laser-Based Strain Measurement on MEMS Materials[J]. Experimental Techniques, 1999, 23(3): 28-30
[26] S. Meyer, E. Diegele, A. Bruckner-Foit, A. Moslang: Crack Interaction Modelling[J]. Fatigue and Fracture of Engineering Materials and Structures, 2000, 23(4): 315-323
[27] Y. Ochi, A. Ishii, S.K. Sasaki: An Experimental and Statistical Investigation of Surface Fatigue Crack Initiation and Growth[J], Fatigue & Fracture of Engineering Materials & Structures. 1985, 8(4): 327-339
[28] Y.M. Hu, W. Floer, U. Krupp, H.-J. Christ: Microstructurally Short Fatigue Crack Initiation and Growth in Ti-6.8Mo-4.5Fe-1.5Al[J]. Materials Science and Engineering A. 2000, 278: 170-180
[29] S. Matsuda, T. Inoue, H. Mimura, Y. Okaura. Proceedings of International Symposium Toward Improved Ductility and Toughness. Kyoto, Japan, 1971: 45-46
[30] Tadashi MAKI; Kaneaki TSUZAKI; Imao TAMURA. The Morphology of Microstructure Composed of Lath Martensites in Steels[J]. Transactions of the Iron and Steel Institute of Japan, 2019, 20(4): 207-214
[31] G. Krauss, Mater. Sci. Eng. A273-275(1999): 40-57.